

COMPARISON OF OBSERVED SURFACE TEMPERATURES OF 4 VETSA TO THE KRC THERMAL MODEL. T. N. Titus¹, K. J. Becker¹, J. A. Anderson¹, M.T. Capria², F. Tosi², M.C. De Sanctis², E. Palomba², D. Grassi², F. Capaccioni², E. Ammannito², J.-P. Combe³, T.B. McCord³, J.-Y. Li⁴, C.T. Russell⁵, C.A. Raymond⁶, D. Mittlefehldt⁷, M. Toplis⁸, O. Forni⁹, M.V. Sykes¹⁰. ¹Astrogeology Science Center, U.S. Geological Survey, 2255 North Gemini Drive, Flagstaff, AZ 86001, USA, ttitus@usgs.gov. ²INAF-IAPS, Via del Fosso del Cavaliere 100, I-00133 Rome, Italy. ³Bear Fight Institute, 22, Fiddler's Road, P.O. Box 667, Winthrop, WA, 98862, USA. ⁴Department of Astronomy, University of Maryland at College Park, MD 20742-2421, USA. ⁵Institute of Geophysics and Planetary Physics, University of California at Los Angeles, 3845 Slichter Hall, 603 Charles E. Young Drive, East, Los Angeles, CA 90095-1567, USA. ⁶NASA/Jet Propulsion Laboratory and California Institute of Technology, 4800 Oak Grove Drive, Pasadena, CA 91109, USA. ⁷NASA Johnson Space Center, 2101 NASA Parkway, Houston, TX 77058, USA. ⁸Institut de Recherche en Astrophysique et Planétologie (UMR 5277), Observatoire Midi-Pyrénées, 31400, Toulouse, France. ⁹Institut de Recherche en Astrophysique et Planétologie, 9, avenue du Colonel Roche - BP 4346, 31028 Toulouse Cedex 4, France. ¹⁰Planetary Science Institute, 1700 E. Fort Lowell, Suite 106, Tucson, AZ 85719, USA.

Introduction: In this work, we will compare observed temperatures of the surface of Vesta using data acquired by the Dawn [1] Visible and Infrared Mapping Spectrometer (VIR-MS) [2] during the approach phase to model results from the KRC thermal model.

Thermal Inertia: Thermal inertia (I) is a measure of how quickly a material responds to changes in temperature and is defined as $I = \sqrt{k\rho c}$, where k is the thermal conductivity, ρ is the bulk density, and c is the specific heat capacity. SI units for I are $\text{J m}^{-2} \text{s}^{-1/2} \text{K}^{-1}$ which henceforth will be referred to as "TIU" (thermal inertia unit) as proposed by Putzig [3].

High thermal inertia materials, such as bedrock, resist changes in temperature while temperatures of low thermal inertia material, such as dust, respond quickly to changes in solar insolation. The surface of Vesta is expected to have low to medium thermal inertia values, with the most commonly used value being extremely low at 15 TIU [4].

There are several parameters which affect observed temperatures in addition to thermal inertia: bond albedo, slope, and surface roughness. In addition to these parameters, real surfaces are rarely uniform monoliths that can be described by a single thermal inertia value. Real surfaces are often vertically layered or are mixtures of dust and rock. For Vesta's surface, with temperature extremes ranging from 50 K to 275 K and no atmosphere, even a uniform monolithic surface may have non-uniform thermal inertia due to temperature dependent thermal conductivity.

KRC Thermal Model: We employ a multi-layered thermal-diffusion model called 'KRC' [5], which has been used extensively in the study of Martian thermal physical properties [e.g. 5-11]. This thermal model is easily modified for use with Vesta by replacing the martian ephemeris input with the Vesta ephemeris and turning the atmosphere off. This model calculates surface temperatures throughout an entire

Vesta year for a specific set of slope, azimuth, latitude, elevation and albedo for up to ten different thermal inertia values. To calculate surface temperatures, KRC uses the Delta-Eddington approximation for radiative flux (Kieffer et al., 1977) to solve the subsurface thermal diffusion equation using finite-difference methods. The upper boundary condition is solar insolation (calculated at each step according to orbital position, orbital inclination and time of day). KRC models are run with varying values for albedo, thermal inertia and layer depth to create temperature indices which are closely matched, via bilinear interpolation, to the dates and times observed by VIR. After this interpolation, our working index contains modeled temperatures for all times of observation at a logarithmic range of ten thermal inertias between 15 and 400 TIU. Higher values of TIU can be included if necessary. The downhill-simplex method of function minimization (Nelder and Mead, 1986) is then used to compare the observed and modeled data to determine best-fit values for thermal inertia (and layer depth when applicable).

Vesta Approach Data: The Dawn spacecraft [1] acquired approach observations on June 30, 2011. Figure 1 shows a false-color view of Vesta as seen by VIR in the near-infrared. These data provide full disk view of Vesta, providing a range of local times (Fig 2).



Figure 1: VIR IR False color image.

Vesta Temperature Data: Temperatures were calculated using a Bayesian approach to nonlinear inversion as described by Tosi et al. [13, 14]. In order to compare observed temperatures of Vesta to model calculations, several geometric and photometric param-

ters must be known or estimated. These include local mean solar time, latitude, local slope, bond bolometric albedo, and the effective emissivity at $5\mu\text{m}$. Local time, latitude, and local slope are calculated using the USGS ISIS [15, 16] software system. The bolometric bond albedo is estimated from the observed surface reflectivity. The effective emissivity is estimated by comparing the total radiance at $5\mu\text{m}$ to the solar flux and the thermal emission. If one assumes that Kirchhoff's Law applies and that the surface reflection can be approximated as Lambertian, then the observed radiance (R_{obs}) is a function of emissivity:

$$R_{obs} = (1 - A_\lambda)\mu_o \square_{sol} + \epsilon_\lambda \beta_\lambda(T) = \epsilon_\lambda (\mu_o \square_{sol} + \beta_\lambda(T))$$

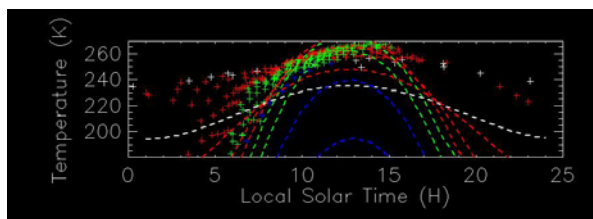


Figure 2: Comparison of observed temperatures to KRC model results assuming a smooth flat surface. The plus signs are VIR temperatures and the dashed lines are the KRC models. The colors indicate latitude where white is 80°S, red is the latitude range 75°S to 20°S, green is the latitude range 20°N to 20°S and blue is the latitude range 20°N to 60°N.

Roughness Effects: Because KRC is a 1-D model, the effects of roughness are approximated by combining a suite of KRC model results with a range of slopes and slope azimuths. While this approach captures many of the effects of surface roughness, it does not correct for the secondary effects of radiative coupling between facing surfaces of varying temperatures.

Results: Figure 2 compares the observed temperatures to KRC model results assuming a smooth flat surface with a fixed bond albedo of 0.2 and a surface emissivity of 0.6. The model curves shown are for a thermal inertia of 30 TIU. The need to incorporate surface roughness is clearly illustrated. The temperature profiles as a function of latitude and local time of day are generally the correct shape, but effects from beaming and surface roughness are needed to properly model the warm temperatures observed.

Future Work: The incorporation of local slopes, emissivity, and albedo is the next step in this project.

Conclusion: Thermal inertia analysis of the surface of Vesta has great potential to identify a variety of processes ranging from variations in grain size to effects of cementation.

Acknowledgements: We would like to thank the efforts of Hugh Kieffer for his help modifying KRC parameters to work with Vesta. This work has greatly benefited from the comments and suggestions of several people, including Rose Hayward and Oleg Abramov. This work is supported by NASA's Dawn at Vesta Participating Scientist grant number NNX11AC28G.

References: [1] C.T. Russell, et al., *Planetary and Space Science*, 52, 465–489, 2004. [2] De Sanctis, M.C., et al. (2010). *Space Sci. Rev.*, doi: 10.1007/s11214-010-9668-5. [3] N. E. Putzig (2006) Ph.D. Dissertation. [4] Spencer (1990) *Icarus*, 83, 27–38. [5] Kieffer et al., (1977) *JGR*, 82, 4249–4291. [6] Titus et al. (2003) *Sci.*, 299, 1048–1051. [7] Kirk et al., (2004) *Photogramm. Eng. Remote Sens.*, 71(10), 1167–1178. [8] R. Fergason et al. 2006, [9] Bandfield & Feldman 2008, [10] G. E. Cushing & T. N. Titus (2008) *JGR*, 113, E06006 [11] Cushing et al. (2009) 114, CiteID E07002 [12] Nelder and Mead, 1986 *Numerical Recipes: The Art of Scientific Computing*, 292–293, Cambridge Univ. Press, New York. [13] Tosi, F., et al. (2012) In preparation. [14] F. Tosi et al. (2012) *LPS XLIII* [15] Anderson, J. A., et al. (2004), *LPSC XXXV*, abstract 2039 [16] K. Becker et al. (2012) *LPS XLIII*.